ISSN: 2277-3754
ISO 9001:2008 Certified
International Journal of Engineering and Innovative Technology (IJEIT)
Volume 3, Issue 3, September 2013

Advances on Robust Control of Civil Engineering Smart Structures

Amalia J. Moutsopoulou, Georgios E. Stavroulakis, Anastasios Pouliezos

***Abstract*— this paper develops a robust active control approach with parametric uncertainties in smart structures. Large amplitudes and attenuating vibration periods result in fatigue, instability, and poor structural performance. In light of past research in this field, this paper intends to discuss some innovative approaches in vibration control of smart structures, particularly in the case of structures with embedded piezoelectric materials. More advanced theories for control strategies are presented, such as robust control theory and uncertainty modeling. The resulting approach to robust control may be applied for the analysis and design of practical smart structures.**

***Index Terms*—D_K iterative method, H_∞performance, Robust active control, Smart structures, Uncertain structural systems.**

I. INTRODUCTION

Slender structures and long bridges that inherit numerous uncertainties due to model errors, simplified assumptions in stress calculations, material properties, and load environments, may undergo large forces from natural hazards such as earthquakes and strong wind events. The robust control method provides robust relative stability, the $H\infty$ norm of the transfer function from the external disturbance forces (e.g., earthquake, wind, etc.) to the observed smart structures states is restricted by a prescribed attenuation index. The smart structures have broadly motivated research interest during the last decades [1]-[10]. A smart structure would be able to sense the vibration and generate a controlled actuation so that the vibration can be minimized [1]. The stimulus to a structure may originate from external disturbances e.g., earthquake, wind, or excitations that cause good broadband sensing and actuation properties [1]. The ability of piezoelectric materials to exchange electrical and mechanical energy opens up the possibility of employing them as actuators and sensors. If the piezoelectric materials are bonded properly to a structure, structural deformations can be induced by applying a voltage to the materials, employing them as actuators. On the other hand, they can be employed as sensors since deformations of a structure would cause the deformed. piezoelectric materials produce an electric charge [6], [7]. The extent of structural deformation can be observed by measuring the electrical voltage that the materials produce [9], [10]. A short literature review gives a deep insight into the research work done on the intelligent structures so far. Culshaw [11] discussed the concept of smart structure, its benefits and applications. Rao and Sunar explained the use of piezo materials as sensors and actuators in sensing vibrations in their survey paper [12]. Hubbard and Baily [13] have studied the application of piezoelectric materials as sensor / actuator for flexible structures. Hanagud et.al. [14] developed a Finite Element Model (FEM) for a beam with many distributed piezoceramic sensors / actuators. Hwang and Park [15] presented a new finite element (FE) modeling technique for flexible beams. Continuous time and discrete time algorithms were proposed to control a thin piezoelectric structure by Bona, et.al. [16]. Schiehlen and Schonerstedt [17] reported the optimal control designs for the first few vibration modes of a cantilever beam using piezoelectric sensors / actuators. S.B. Choi et.al. [18] have shown a design of position tracking sliding mode control for a smart structure. Distributed controllers for flexible structures can be seen in Forouza Pourki [19]. A FEM approach was used by Benjeddou et.al. [20] to model a sandwich beam with shear and extension piezoelectric elements. The finite element model employed the displacement field of Zhang and Sun [21]. It was shown that the finite element results agree quite well with the analytical results. Raja et.al. [22] extended the finite element model of Benjeddou's research team to include a vibration control scheme. In this paper we introduce uncertainties in smart structures. The control system aims at suppressing undesirable ones and/or enhancing desirable effects. We study an example of such a structure: an intelligent beam with integrated piezoelectric actuators, the goal of which is to suppress oscillations under stochastic loads. First we examine the H_∞ criterion which takes into account the worst case scenario of uncertain disturbances or noise in the system. Therefore, it is possible to synthesize a H_∞ controller which will be robust with respect to a predefined number of uncertainties in the model. By using uncertainties one may take into account non-linearity of the structure, damage or other changes from the nominal model, and, subsequently, analyse and design a robust-controller. The results are very good: the oscillations were suppressed even for a real Aeolian-type load, with the voltages of the piezoelectric components laying within their endurance limits.

II. MATHEMATICAL MODELING

A cantilever slender beam with rectangular cross-sections is considered. Four pairs of piezoelectric patches are embedded symmetrically at the top and the bottom surfaces of the beam, as shown in Fig. 1.

ISSN: 2277-3754
ISO 9001:2008 Certified
International Journal of Engineering and Innovative Technology (IJEIT)
Volume 3, Issue 3, September 2013

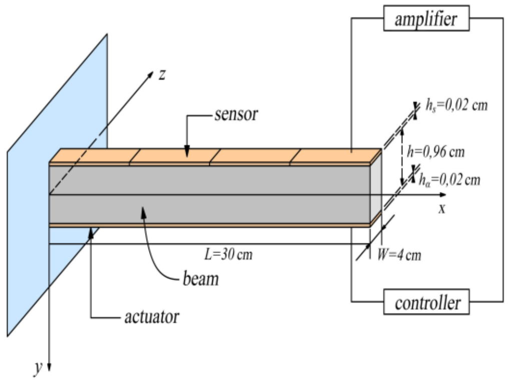

Fig.1 Smart Beam

The beam is from graphite- epoxy T300 − 976 and the piezoelectric patches are PZT G1195N. The top patches act like sensors and the bottom like actuators. The resulting composite beam is modeled by means of the classical laminated technical theory of bending. Let us assume that the mechanical properties of both the piezoelectric material and the host beam are independent in time. The thermal effects are considered to be negligible as well [8]. The beam has length *L*, width *W* and thickness *h*. The sensors and the actuators have width b_S and b_a and thickness h_S and h_a, respectively. The electromechanical parameters of the beam of interest are given in the table 1.

Table 1: Parameters Of The Composite Beam.

Parameters	Values
Beam length, *L*	0.3 m
Beam width, *W*	0.04 m
Beam thickness, *h*	0.0096 m
Beam density, *ρ*	1600 kg/m^3
Youngs modulus of the beam, *E*	1.5 X 10^{11} N/m^2
Piezoelectric constant, d_{31}	254 X 10^{-12} m/V
Electric constant, ξ_{33}	11.5 X 10^{-3} V m/N
Young's modulus of the piezoelectric element	1.5 X 10^{11} N/m^2
Width of the piezoelectric element	$b_S = b_a = 0.04$ m
Thickness of the piezoelectric element	$h_S = h_a = 0.0002$ m

In order to derive the basic equations for piezoelectric sensors and actuators [1], we assume that:

- The piezoelectric sensors actuators (S/A) are bonded perfectly on the host beam;
- The piezoelectric layers are much thinner then the host beam;
- The piezoelectric material is homogeneous, transversely isotropic and linearly elastic;
- The piezoelectric sensors actuators (S/A) are transversely polarized [1].

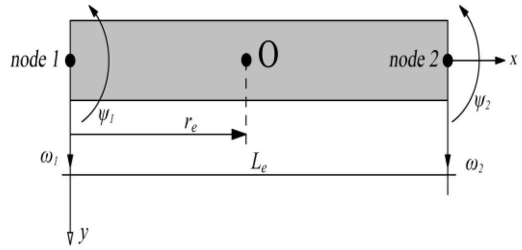

Fig. 2: Beam finite element

A. *Finite Element Formulation*

We consider a beam element of length *Le*, which has two mechanical degrees of freedom at each node: one translational ω_1 (respectively ω_2) in direction z and one rotational φ_1 (respectively φ_2), as it is shown in Fig. 2. The vector of nodal displacements and rotations q_e is defined as [23],

$$q_e^r = [\omega_1, \psi_1, \omega_2, \psi_2] \tag{1}$$

The beam element transverse deflection $\omega(x,t)$ and the beam element rotation $\psi(x, t)$ of the beam are continuous and they are interpolated within by Hermitian linear shape functions H_i^{ω} and H_i^{ψ} as follows [11],

$$\omega(x,t) = \sum_{i=1}^{4} H_i^{\omega}(x) q_i(t)$$
$$\psi(x,t) = \sum_{i=1}^{4} H_i^{\psi}(x) q_i(t) \tag{2}$$

This classical finite element procedure leads to the approximate discretized variational problem. For a finite element the discrete differential equations are obtained by substituting the discretized expressions 12 into the first variation of the kinetic energy and strain energy [5], [6] to evaluate the kinetic and strain energies. Integrating over spatial domains and using the Hamiltons principle [5], the equation of motion for a beam element are expressed in terms of nodal variable q as follows,

$$M\ddot{q}(t) + D\dot{q}(t) + Kq(t) = f_m(t) + f_e(t) \tag{3}$$

where *M* is the generalized mass matrix, *D* the viscous damping matrix, *K* the generalized stiffness matrix, f_m the external loading vector and f_e the generalized control force vector produced by electromechanical coupling effects. The independent variable $q(t)$ is composed of transversal deflections ω_1 and rotations ψ_1, i.e., [6]

$$q(t) = \begin{bmatrix} \omega_1 \\ \psi_1 \\ \vdots \\ \omega_n \\ \psi_n \end{bmatrix} \tag{4}$$

Where *n* is the number of nodes used in analysis. Vectors *ω* and f_m are positive upwards. To transform to state-space control representation, let (in the usual manner),

ISSN: 2277-3754
ISO 9001:2008 Certified
International Journal of Engineering and Innovative Technology (IJEIT)
Volume 3, Issue 3, September 2013

$$\dot{x}(t) = \begin{bmatrix} q(t) \\ \dot{q}(t) \end{bmatrix} \tag{5}$$

Furthermore to express $f_e(t)$ as $Bu(t)$ we write it as $f_e^* u$ where f_e^* the piezoelectric force is for a unit applied on the corresponding actuator, and u represents the voltages on the actuators. Furthermore, $d(t) = f_m(t)$ is the disturbance vector [6], the control vector *u(t)* and the disturbance vector *d(t)* are the inputs of our system.

Then,

$$\dot{x}(t) = \begin{bmatrix} O_{2n\times 2n} & I_{2n\times 2n} \\ -M^{-1}K & -M^{-1}D \end{bmatrix} x(t) + \begin{bmatrix} O_{2n\times 2n} \\ M^{-1}f_e^* \end{bmatrix} u(t) + \begin{bmatrix} O_{2n\times 2n} \\ M^{-1} \end{bmatrix} \tag{6}$$

$$= Ax(t) + Bu(t) + Gd(t) = Ax(t) + \begin{bmatrix} B & G \end{bmatrix} \begin{bmatrix} u(t) \\ d(t) \end{bmatrix} = Ax(t) + B\tilde{u}(t)$$

The previous description of the dynamical system will be augmented with the output equation (displacements only measured) [5],

$$y(t) = Cx(t) \tag{7}$$

In this formulation u is $n\ x\ 1$ (at most, but can be smaller), while d is $2n\ x\ 1$. The units used are compatible for instance m, rad, sec and N.

III. DESIGN OBJECTIVES AND SYSTEM SPECIFICATIONS

The structured singular value of a transfer function matrix is defined as,

$$\mu(M) = \begin{cases} \dfrac{1}{\min\limits_{k_m}\{\det(I - k_m M\Delta) = 0, \bar{\sigma}(\Delta) \le 1\}} \\ 0, \text{if no such structured exists} \end{cases} \tag{8}$$

In words it defines the smallest structured *Δ* (measured in terms of $\bar{\sigma}(\Delta)$) which makes *det(I−MΔ)=0*: then $\mu(M) = 1/\bar{\sigma}(\Delta)$. It follows that values of μ smaller than 1 are desired (the smaller the better: a larger variation is allowed) [8], [24].

A. Design Objectives

Design objectives fall into two categories:

1. Stability of closed loop system (plant+controller).

Nominal performance

2. Disturbance attenuation with satisfactory transient characteristics (overshoot, settling time).
3. Small control effort.

Robust performance

4. (1)-(3) above should be satisfied in the face of modeling errors.

B. System specifications

To obtain the required system specifications to meet the above objectives we need to represent our system in the so-called *(N, Δ)* structure. To do this start with the simple typical diagram of Fig. 3.

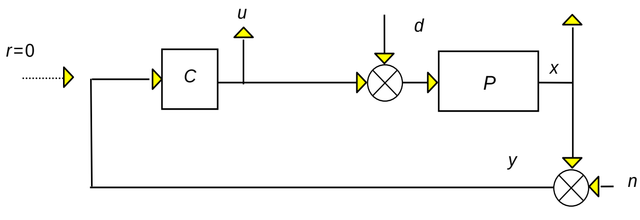

Fig. 3 Classical control block diagram

In this diagram there are two inputs, *d (disturbances)* and *n (noise)*, and two outputs, *u (control vector)* and *x (the state vector)*. In what follows it is assumed that,

$$\left\| \begin{matrix} d \\ n \end{matrix} \right\|_2 \le 1, \quad \left\| \begin{matrix} u \\ x \end{matrix} \right\|_2 \le 1 \tag{10}$$

If that's not the case, appropriate frequency-dependent weights can transform original signals so that the transformed signals have this property.

Rewrite Fig. 3 like Fig.4:

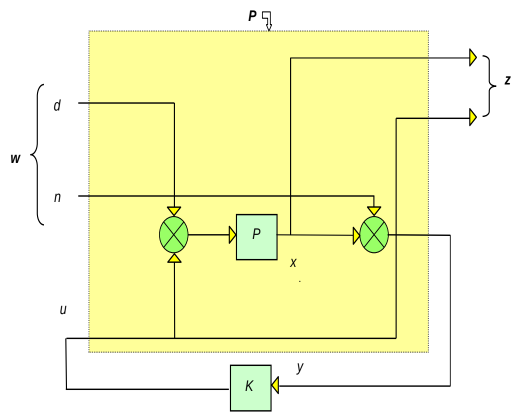

Fig. 4 detailed two-port diagramor in less detail,

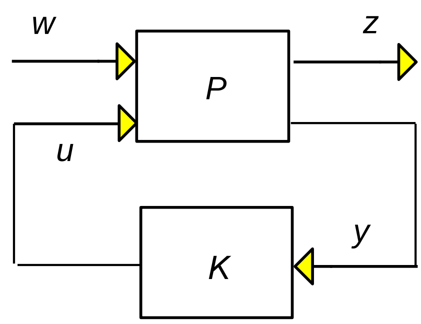

Fig. 5 Two-port diagram

with,

$$z = \begin{bmatrix} u \\ x \end{bmatrix}, \quad w = \begin{bmatrix} d \\ n \end{bmatrix} \tag{11}$$

Where z are the output variables to be controlled, and w the exogenous inputs, P is our system and K is the controller. Fig. 5 and Fig. 6 represent our problem in the state-space form. Given that P has two inputs and two outputs it is, as usual, naturally partitioned as,

ISSN: 2277-3754
ISO 9001:2008 Certified
International Journal of Engineering and Innovative Technology (IJEIT)
Volume 3, Issue 3, September 2013

$$\begin{bmatrix} z(s) \\ y(s) \end{bmatrix} = \begin{bmatrix} P_{zw}(s) & P_{zu}(s) \\ P_{yw}(s) & P_{yu}(s) \end{bmatrix} \begin{bmatrix} w(s) \\ u(s) \end{bmatrix} \overset{op}{=} P(s) \begin{bmatrix} w(s) \\ u(s) \end{bmatrix} \quad (12)$$

Also,

u(s)=K(s)y(s) (13)

The closed loop transfer function $N_{zw}(s)$ is defined by,

Nzw(s)=Pzw(s)+Pzu(s)K(s)(I−Pyu(s)K(s))−1Pyw(s) (14)

To deduce robustness specifications a further diagram is needed, namely that of Fig.6:

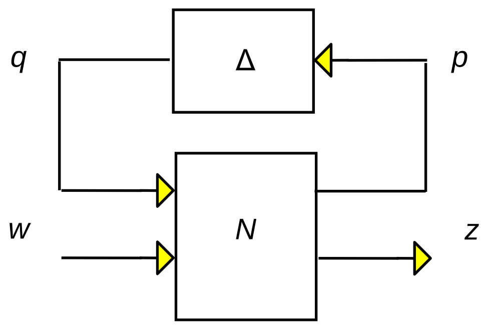

Fig. 6 N-Δ structure for uncertainty modeling

where N is defined by (14) and uncertainty modeled in Δ satisfies $\|\Delta\|_\infty \le 1$ (details later). Here,

$z=\Phi_u(N, \Delta)w=[N_{22}+N_{21}\Delta(I-N_{11}\Delta)^{-1}N_{12}]w=Fw$ (15)

Given this structure we can state the following definitions:

Nominal stability (NS) ⇔	N internally stable
Nominal performance (NP) ⇔	$\|N_{22}(j\omega)\|_\infty<1, \ \forall\omega$ and NS
Robust stability (RS) ⇔	$F=\Phi_u(N, \Delta)$ stable $\forall\Delta, \ \|\Delta\|_\infty<1$ and NS
Robust performance (RP) ⇔	$\|F\|_\infty<1, \ \forall\Delta, \ \|\Delta\|_\infty<1$ and NS

It has been proved that the following conditions hold in the case of block-diagonal real or complex perturbations Δ:

Ⅰ. The system is nominally stable if M is internally stable.

II. The system exhibits nominal performance if

III The system (M, Δ) is *robustly stable* if and only if,

$$\sup_{\omega\in\mathbb{R}} \mu_\Delta\left(N_{11}(j\omega)\right)<1 \quad (16)$$

where μ_Δ is the structured singular value of N given the structured uncertainty set Δ. This condition is known as the generalized small gain theorem.

IV The system (N, Δ) exhibits robust performance if and only if,

$$\sup_{\omega\in\mathbb{R}} \mu_{\Delta_a}\left(N(j\omega)\right)<1 \quad (17)$$

where,

$$\Delta_a = \begin{bmatrix} \Delta_p & 0 \\ 0 & \Delta \end{bmatrix} \quad (18)$$

and Δp is full complex, has the same structure as Δ and dimensions corresponding to *(w, z)*.

Unfortunately, only bounds on μ can be estimated.

C. Controller synthesis

All the above answer the analysis problem and provide tools to judge the performance of any controller and also compare controllers. However it is possible to approximately synthesize a controller that achieves given performance in terms of the structured singular value μ.

In this procedure known as (*D, G-K*) iteration [3[, [24], the problem of finding a μ-optimal controller K such that

$\mu(\Phi_u\ (F(j\omega),\ K(j\omega))\le\beta,\ \ \forall\omega$, is transformed into the problem of finding transfer function matrices $D(\omega)\in\Delta$ and $G(\omega)\in\Gamma$, such that,

$$\sup_{\omega} \bar\sigma\left[\left(\frac{D(\omega)(F_u(F(j\omega),K(j\omega))D^{-1}(\omega)}{\gamma} - jG(\omega)\right)\left(I+G^2(\omega)\right)^{-\frac{1}{2}}\right] \le 1, \forall\omega \quad (19)$$

Unfortunately this method does not guarantee even finding local maxima [25]. It combines H_∞ synthesis and μ-analysis and often yields good results. The starting point is an upper bound on μ in terms of the scaled singular value,

$$\mu(N) \le \min_{D\in D} \bar\sigma(DND^{-1}) \quad (20)$$

The idea is to find the controller that minimizes the peak over frequency of its upper bound, namely,

$$\min_K\left(\min_{D\in D}\left\|DN(K)D^{-1}\right\|_\infty\right) \quad (21)$$

by alternating between minimizing $\left\|DN(K)D^{-1}\right\|_\infty$ with respect to either K or D (while holding the other fixed).

1. *K-step.* Synthesize an H_∞ controller for the scaled problem $\min_K\left\|DN(K)D^{-1}\right\|_\infty$ with fixed *D(s).*

2. *D-step.* Find $D(j\omega)$ to minimize at each frequency $\bar\sigma(DND^{-1}(j\omega))$ with fixed *N.*

3. Fit the magnitude of each element of $D(j\omega)$ to a stable and minimum phase transfer function $D(s)$ and got to Step 1.

D. System uncertainty

The main sources of uncertainty are:

* Nonlinearity and/or dynamic aspects of the system that are ignored at the modeling phase. The error introduced in modal analysis by using only a few significant eigenmodes leads to an uncertainty of the type discussed here.

* Incomplete knowledge of model values and parameters and/or natural fluctuation of those values during system operation.

ISSN: 2277-3754
ISO 9001:2008 Certified
International Journal of Engineering and Innovative Technology (IJEIT)
Volume 3, Issue 3, September 2013

* Influence of the system's environment, in the form of disturbances.

Assume uncertainty in the M and K matrices of the form,

$$K = K_0(I + k_p I_{2n\times 2n}\delta_K) \tag{22}$$
$$M = M_0(I + m_p I_{2n\times 2n}\delta_M) \tag{23}$$

Also, since, D=0.0005(K+M), an appropriate form for D is,

$$D = 0.0005[K_0(I + k_p I_{2n\times 2n}\delta_K) + M_0(I + m_p I_{2n\times 2n}\delta_M)] =$$
$$D_0 + 0.0005[K_0 k_p I_{2n\times 2n}\delta_K + M_0 m_p I_{2n\times 2n}\delta_M] \tag{24}$$

Alternatively, by adopting the well-known Rayleigh damping assumption,

$$D = \alpha K + \beta M \tag{25}$$

D could be expressed similarly to K, M, as,

$$D = D_0(I + d_p I_{2n\times 2n}\delta_D) \tag{26}$$

In this way we introduce uncertainty in the form of percentage variation in the relevant matrices. Uncertainty is most likely to arise from terms outside the main matrices (since length can be adequately measured).

Here it will be assumed,

$$\|\Delta\|_\infty \overset{\text{def}}{=} \left\| \begin{bmatrix} \mathrm{I}_{n\times n}\delta_{\mathrm{K}} & 0_{n\times n} \\ 0_{n\times n} & \mathrm{I}_{n\times n}\delta_{\mathrm{M}} \end{bmatrix} \right\|_\infty < 1 \tag{27}$$

hence mp, kp are used to scale the percentage value and the zero subscript denotes nominal values.

(it is reminded that for matrix A n×m the norm is calculated through $\|A\|_\infty = \max_{1\le j\le m} \sum_{j=1}^{n} |a_{ij}|$)

With these definitions (3) becomes,

$$M_0(I + m_p I_{2n\times 2n}\delta_M)\ddot{q}(t) + K_0(I + k_p I_{2n\times 2n}\delta_K)q(t) +$$
$$+[D_0 + 0.0005[K_0 k_p I_{2n\times 2n}\delta_K + M_0 m_p I_{2n\times 2n}\delta_M]]\dot{q}(t) = f_m(t) + f_e(t) \tag{28}$$

$$\Rightarrow M_0\ddot{q}(t) + D_0\dot{q}(t) + K_0 q(t) =$$
$$-[M_0 m_p I_{2n\times 2n}\delta_M \ddot{q}(t) + 0.0005[K_0 k_p I_{2n\times 2n}\delta_K + M_0 m_p I_{2n\times 2n}\delta_M]\dot{q}(t)$$
$$+K_0 k_p I_{2n\times 2n}\delta_K q(t)] + f_m(t) + f_e(t) \tag{29}$$
$$\Rightarrow M_0\ddot{q}(t) + D_0\dot{q}(t) + K_0 q(t) = \tilde{D}q_u(t) + f_m(t) + f_e(t) \tag{30}$$

where,

$$q_u(t) = \begin{bmatrix} \ddot{q}(t) \\ \dot{q}(t) \\ q(t) \end{bmatrix} \tag{31}$$

$$\tilde{D} = -[M_0 m_p \quad K_0 k_p] \begin{bmatrix} I_{2n\times 2n}\delta_M & 0_{2n\times 2n} \\ 0_{2n\times 2n} & I_{2n\times 2n}\delta_K \end{bmatrix} \begin{bmatrix} I_{2n\times 2n} & 0.0005 I_{2n\times 2n} & 0_{2n\times 2n} \\ 0_{2n\times 2n} & 0.0005 I_{2n\times 2n} & I_{2n\times 2n} \end{bmatrix} =$$
$$= G_1 \cdot \Delta \cdot G_2 \tag{32}$$

Writing in state space form, gives,

$$\dot{x}(t) = \begin{bmatrix} 0_{2n\times 2n} & I_{2n\times 2n} \\ -M^{-1}K & -M^{-1}D \end{bmatrix} x(t) + \begin{bmatrix} 0_{2n\times n} \\ M^{-1}f_e^* \end{bmatrix} u(t)$$
$$+ \begin{bmatrix} 0_{2n\times 2n} \\ M^{-1} \end{bmatrix} d(t) + \begin{bmatrix} 0_{2n\times 6n} \\ M^{-1}G_1\cdot\Delta\cdot G_2 \end{bmatrix} q_u(t)$$
$$= Ax(t) + Bu(t) + Gd(t) + G_u G_2 q_u(t) \tag{33}$$

In this way we treat uncertainty in the original matrices as an extra uncertainty term.

To express our system in the form of Fig. 6, consider in the frequency domain Fig. 7.

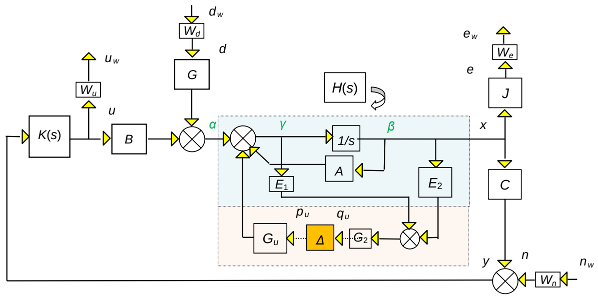

Fig. 7 Uncertainty block diagram

This diagram is the weighted block diagram in the frequency domain. W_d, W_e, W_u, W_n are the weight of the disturbances, errors, control, noise. *H(s)* is our system, *K(s)*, is the controller and Δ define the uncertainties.

The matrices E_1, E_2 are used to extract,

$$q_u(t) \overset{\text{def}}{=} \begin{bmatrix} \ddot{q}(t) \\ \dot{q}(t) \\ q(t) \end{bmatrix} \tag{34}$$

Since,

$$\gamma = \begin{bmatrix} \dot{q}(t) \\ \ddot{q}(t) \end{bmatrix} \quad \text{and} \quad \beta = \int \begin{bmatrix} \dot{q}(t) \\ \ddot{q}(t) \end{bmatrix} \mathrm{d}t = \begin{bmatrix} q(t) \\ \dot{q}(t) \end{bmatrix} \tag{35}$$

appropriate choices for E1, E2 are,

$$E_1 = \begin{bmatrix} 0_{2n\times 2n} & I_{2n\times 2n} \\ I_{2n\times 2n} & 0_{2n\times 2n} \\ 0_{2n\times 2n} & 0_{2n\times 2n} \end{bmatrix}, \quad E_2 = \begin{bmatrix} 0_{2n\times 2n} & 0_{2n\times 2n} \\ 0_{2n\times 2n} & 0_{2n\times 2n} \\ I_{2n\times 2n} & 0_{2n\times 2n} \end{bmatrix} \tag{36}$$

The idea is to find an N such that,

$$\begin{bmatrix} q_u \\ e_w \\ u_w \end{bmatrix} = N \begin{bmatrix} p_u \\ d_w \\ n_w \end{bmatrix},$$
$$N = \begin{bmatrix} N_{p_u q_u} & N_{d_w q_u} & N_{n_w q_u} \\ N_{p_u e_w} & N_{d_w e_w} & N_{n_w e_w} \\ N_{p_u u_w} & N_{d_w u_w} & N_{n_w u_w} \end{bmatrix} = \begin{bmatrix} N_{11} & N_{12} \\ N_{21} & N_{22} \end{bmatrix} \tag{37}$$

or in the notation of Fig. 6,

$$\begin{bmatrix} q_u \\ w \end{bmatrix} = N \begin{bmatrix} p_u \\ z \end{bmatrix} \tag{38}$$

We'll use a methodology known as "pulling out the Δ's".

ISSN: 2277-3754
ISO 9001:2008 Certified
International Journal of Engineering and Innovative Technology (IJEIT)
Volume 3, Issue 3, September 2013

To this end, break the loop at points p_u, q_u (which will be used as additional inputs/outputs respectively) and use the auxiliary signals α, β and γ.

To get the transfer function $N_{d_w q_u}$ (from d_w to q_u):

$$q_u = G_2(E_2\beta + E_1\gamma) = G_2(E_2 + E_1)\gamma \tag{39}$$

$$\gamma = GW_d d_w + Bu + A\gamma = GW_d d_w + BKC\gamma + A\gamma$$

$$\Rightarrow \gamma = (I - BKC - A)^{-1} GW_d d_w \tag{40}$$

Hence,

$$N_{d_w q_u} = G_2(E_2\frac{1}{s} + E_1)(I - BKC\frac{1}{s} - A\frac{1}{s})^{-1} GW_d$$

Now, $N_{p_u q_u}$, $N_{p_u e_w}$, $N_{p_u u_w}$, are similar to $N_{d_w q_u}$, $N_{d_w e_w}$, $N_{d_w u_w}$ with GW_d replaced by G_u, i.e.,

$$N_{p_u q_u} = G_2(E_2\frac{1}{s} + E_1)(I - BKC\frac{1}{s} - A\frac{1}{s})^{-1} G_u$$

$$N_{p_u e_w} = W_y JH[I + B[K(I - CHBK)^{-1} CH]G_u \tag{41}$$

$$M_{p_u u_w} = W_u K(I - CHBK)^{-1} CHG_u$$

Finally to find $N_{n_w q_u}$,

$$q_u = G_2(E_2\beta + E_1\gamma) = G_2(E_2\frac{1}{s} + E_1)\gamma \tag{42}$$

$$\gamma = Bu + A\frac{1}{s}\gamma = BK\left(W_n n_w + y\right) + A\frac{1}{s}\gamma = BKW_n n_w + BKC\frac{1}{s}\gamma + A\frac{1}{s}\gamma$$

$$\Rightarrow \gamma = (I - BKC\frac{1}{s} - A\frac{1}{s})^{-1} BKW_n n_w \tag{43}$$

Hence,

$$N_{n_w q_u} = G_2(E_2\frac{1}{s} + E_1)(I - BKC\frac{1}{s} - A\frac{1}{s})^{-1} BKW_n \tag{44}$$

Collecting all the above yields N:

$$\begin{bmatrix} G_2\left(E_2\frac{1}{s} + E_1\right)\left(I - BKC\frac{1}{s} - A\frac{1}{s}\right)^{-1} G_u & G_2\left(E_2\frac{1}{s} + E_1\right)\left(I - BKC\frac{1}{s} - A\frac{1}{s}\right)^{-1} GW_d & G_2\left(E_2\frac{1}{s} + E_1\right)\left(I - BKC\frac{1}{s} - A\frac{1}{s}\right)^{-1} BKW_n \\ W_e JH\left[I + BK(I - CHBK)^{-1} CF\right]G_u & W_e J(I - HBKC)^{-1} HGW_d & W_e J(I - HBKC)^{-1} HBKW_n \\ W_u K(I - CHBK)^{-1} CFG_u & W_u (I - KCHB)^{-1} KCHGW_d & W_u (I - KCHB)^{-1} KW \end{bmatrix} \tag{45}$$

Having obtained N for the beam problem, all proposed controllers *K(s)* can be compared using the structured singular value relations.

IV. ROBUSTNESS ISSUES

Methods for the design of robust control laws that take into account non-parametric and unstructured uncertainty take advantage of the properties of the H_∞ norm, and constitute what is known as the H_∞ [26], [27], [28] approximation. A considerable volume of research has been dedicated to this since the beginning of the 1980s, the first being Zames [29], where the minimization of the H_∞ norm of the sensitivity function of a linear closed system is used. In this way, robust stabilization and disturbance rejection problems are solved [26], even in the time domain [30]. The H_∞ approximation is based on the small-gain theorem. Its goal is to find a stabilizer K that stabilizes system P and satisfies the small-gain condition, which is expressed as the value of the $H\infty$ norm of the transfer Tzw between output z and extrinsic input w [9], [10]. The main problem is stated as follows: Find a class of stabilizers that ensure internal stability of the closed system and satisfy the condition $\|Tzw\|_\infty < \gamma$, where γ is a given positive scalar quantity. This problem is suboptimal, because what is sought is not to minimize the H_∞ norm of transfer function Tzw, but to attain a value below a given γ. To solve this problem, the usual approach involves parametrization of the stabilizer class, as proposed by several methods. The most applicable of these methods from a numerical standpoint is the state space method, as it leads either to Riccati equations, or to linear matrix inequalities [27].

The following three steps are taken into account in robust analysis:

i. Define a mathematical model for uncertainty.

ii. Check whether the system is stable within the bounds of uncertainty.

iii. Examine whether the system, if stable, exhibits desirable performance.

The superiority of H_∞ control lies in its ability to take explicitly into account the worst effect of unknown disturbances and noise in the system. Furthermore, at least in theory, it is possible to synthesize an H_∞ controller that is robust to a prescribed amount of modeling errors. Unfortunately, this last possibility is not implementable in some cases, as it will be subsequently illustrated. [8]. In what follows, the robustness to modeling errors of the designed H_∞ controller will be analyzed. In all simulations, routines from Matlab's Robust Control Toolbox will be used. In particular:

1. For uncertain elements,

2. To calculate bounds on the structured singular value,

Numerical models used in all simulations, are implemented in three ways:

1. Through Eq.,(6) with,

$$K = K_0(I + k_p\delta_K)$$

$$M = M_0(I + m_p\delta_M)$$

$$D = D_0 + 0.0005[K_0 k_p I_{2n\times 2n}\delta_K + M_0 m_p I_{2n\times 2n}\delta_M]$$

and subsequent evaluation of matrix N for specific values of k_p, m_p.

2. By use of Matlab's "uncertain element object". As explained, this form is needed in the D-K robust synthesis algorithm.

3. By Simulink implementation of Fig. 7.

V. INPUTS- RESULTS

A typical wind load (Fig. 8) acting on the side of the structure. The wind load is a real life wind speed measurements in relevance with time that took place in Estavromenos of Heraklion Crete. We transform the wind speed in wind pressure with; Loading corresponds to the wind excitation. The function fm(t) has been obtained from the

ISSN: 2277-3754
ISO 9001:2008 Certified
International Journal of Engineering and Innovative Technology (IJEIT)
Volume 3, Issue 3, September 2013

wind velocity record, through the relation

$$f_m(t) = \frac{1}{2}\rho C_u V^2(t) \quad (46)$$

where V=velocity, ρ=density and C_u=1.2.

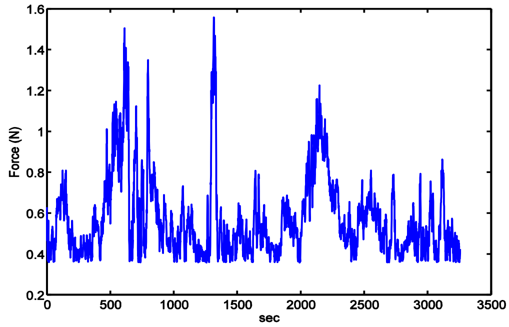

Fig.8 wind load

Moreover, in all simulations, random noise has been introduced to measurements at system output locations within a probability interval of ±1%. Due to small displacements of system nodal points, noise amplitude is taken to be small, of the order of 5 × 10^{-5}. On the other hand, the signal is introduced at each node of the beam by a different percentage, that percentage being lower at the first node due to the fact that the beam end point is clamped. The controller obtained by applying H_∞ control has an order equal to 36. For this controller, γ = 0.074<1. A plot of the maximum singular value of the weighted closed-loop system (beam plus H_∞ controller) is given in Fig. 9, where we can clearly note that the value remains below γ at all frequencies.

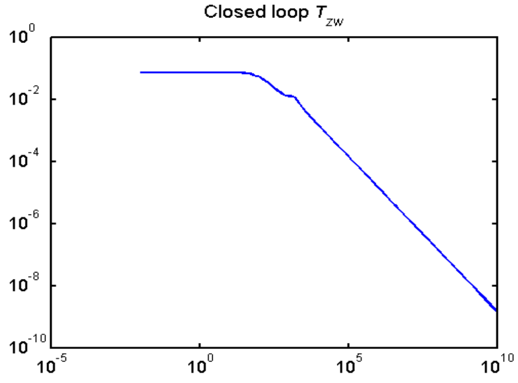

Fig. 9 Maximum singular value of the closed-loop system

Fig. 10 presents the Bode diagrams of diagonal elements of the above weight matrices. These matrices have been obtained through a number of tests, to ensure feasibility of finding a controller H_∞.

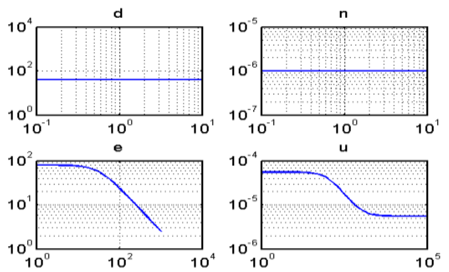

Fig. 10 Bode diagram

Figures 11 a b, further show the maximum singular values of transfer functions of the closed-loop system (i.e. the initial one).

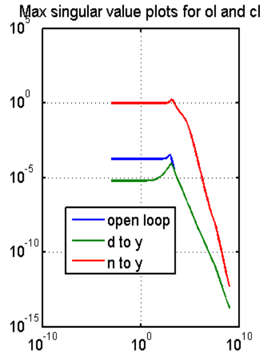

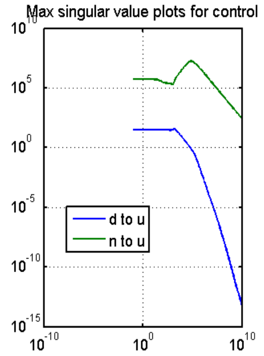

Fig. 11a, b Max singular values

These figures show that the performance of the computed controller is satisfactory, since:

1) As shown in Fig. 11a, there is a significant improvement in the effect of disturbance on error up to the frequency of 1000 Hz.

2) As shown in Fig. 11a, there seems to be little effect of noise on error for frequencies beyond 1000 Hz.

3) Fig. 11b, shows a satisfactory effect of the disturbance on the size of the control scheme (the design could be improved, if it were possible to reduce noise effect for frequencies of 1000 Hz).

To validate the above findings, system response time histories for the three input cases mentioned in this section are presented below in session 5 (Fig. 18, 19).

VI. RESULTS FOR ROBUST ANALYSIS

Robust analysis is carried out through the relations:

$$\sup_{\omega \in \mathrm{R}} \mu_{\Delta}\left(N_{11}(\mathrm{j}\omega)\right) < 1$$

(for robust stability), and,

$$\sup_{\omega \in \mathrm{P}} \mu_{\Delta_a}\left(N(\mathrm{j}\omega)\right) < 1$$

for robust performance

For the H_∞ found, robust analysis was performed for the following values of m_p,k_p.

1. m_p = 0, k_p = 0.9. This corresponds to a ±90% variation from the nominal value of the stiffness matrix K. In Fig. 12 are shown the bounds on the μ values. As seen the system remains stable and exhibits robust performance, since the upper bounds of both values remain below 1 for all frequencies of interest. This result is validated in Fig. 13, where the displacement of the free end and the voltage applied are shown at the extreme uncertainty. Comparison with the open loop response for the same plant shows the good performance of the H_∞ controller. Results are very good, and the beam remains in equilibrium even under realistic wind conditions. Reduction of vibrations is observed, while piezoelectric add-ons produce voltage within their tolerance limits(± 500volt)

ISSN: 2277-3754
ISO 9001:2008 Certified
International Journal of Engineering and Innovative Technology (IJEIT)
Volume 3, Issue 3, September 2013

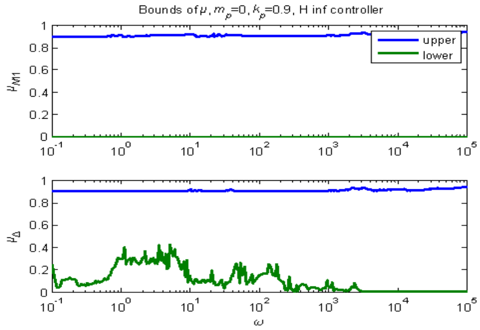

Fig. 12 μ-bounds o H_∞ the controller for mp=0, kp=0.9

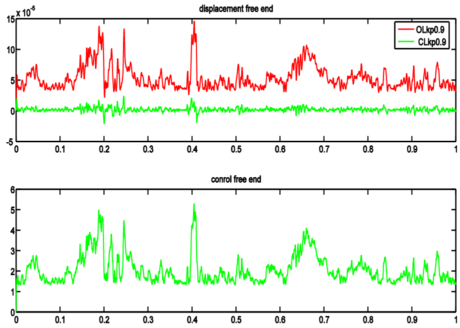

Fig. 13 Displacement and control at free end for the H_∞ controller with mp = 0, kp =0.9 (extreme values)

2. m_p = 0.9, k_p = 0. This corresponds to a ±90% variation from the nominal value of the mass matrix M. In Fig. 14 are shown the bounds on the μ values. As seen the system remains stable and exhibits robust performance, since the upper bounds of both values remain below 1 for all frequencies of interest. This result is validated in Fig. 15, where the displacement of the free end and the voltage applied are shown. Comparison with the open loop response for the same plant shows the good performance of the controller. By employing the H_∞ control, vibration reduction is achieved, while the voltage applied is significantly lower that 500 V.

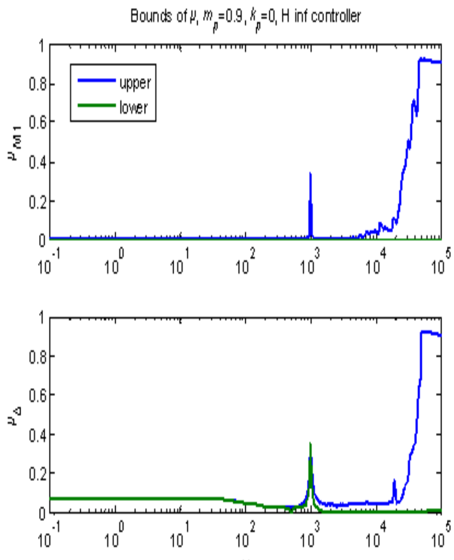

Fig. 14 μ-bounds of the H_∞ controller for mp =0.9, kp =0.

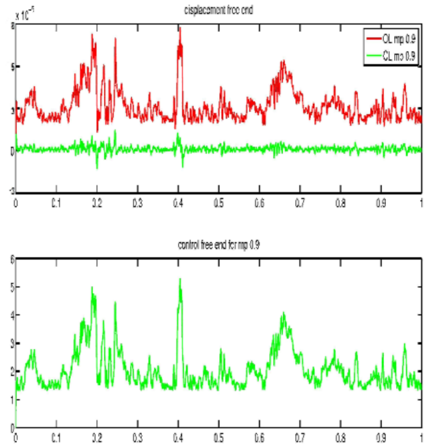

Fig. 15 Displacement and control at free end for the H_∞ controller with *mp* =0.9, *kp* =0 (extreme values)

3. m_p = 0.9, k_p = 0.9. This corresponds to a ±90% variation from the nominal values of both the mass and stiffness matrices M, K.In Fig. 16 are shown the bounds on the μ values. As seen the system remains stable and exhibits robust performance, since the upper bounds of both values remain below 1 for all frequencies of interest. This result is validated in Fig. 17, where the displacement of the free end and the voltage applied are shown. Comparison with the open loop response for the same plant shows the good performance of the controller. Results are very good, and the beam remains in equilibrium even under realistic wind conditions. Reduction of vibrations is observed, while piezoelectric add-ons produce voltage within their tolerance limits.

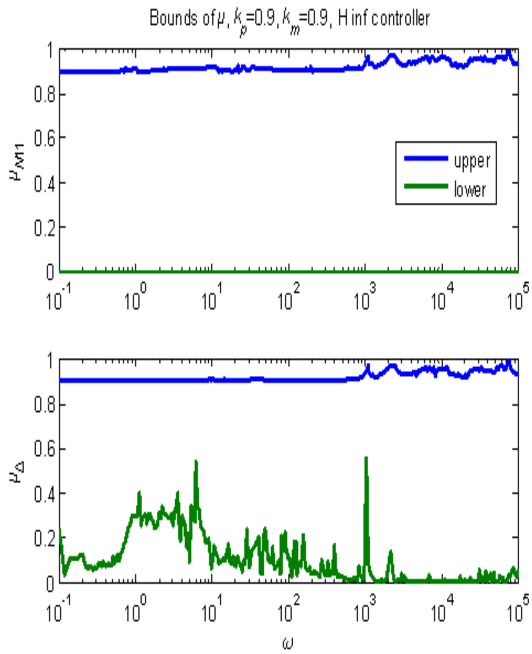

Fig. 16 Displacement and control at free end for the H_∞ controller with mp =0.9, kp =0 (extreme values)

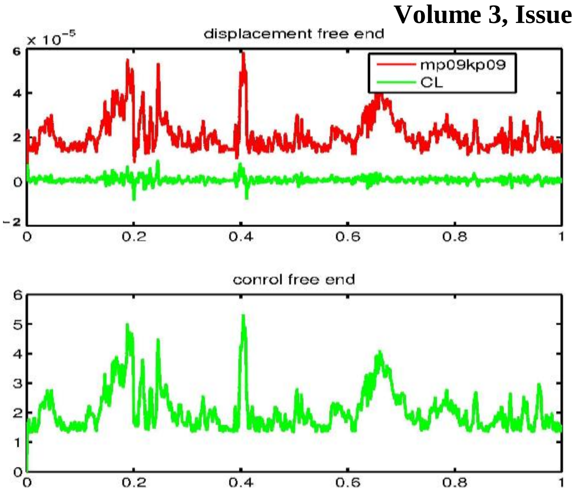

Fig.17 Displacement and control at free end for the H_∞ controller with mp =0.9, kp =0 (extreme values)

Furthermore, we control the structure with variations of the nominal values of the mass matrix *M*, stiffness matrix *K* and matrices *A* and *B*. We take into consideration nonlinearities and system dynamics neglected in modeling, incomplete knowledge of disturbances, environment influence in the form of disturbances, and unreliability of system sensor measurements. In Fig.18α,β complete vibration reduction is achieved even for variations of beam mass and stiffness up to 50%. The piezoelectric force is in their endurance limits, less 500 Volt, Fig 18c. In Fig 19a,b complete vibration reduction is achieved even for variations of matrices *A* and *B* up to 50%. Moreover, controller size contains so as to lower energy consumption and maintain piezoelectric materials within operation limits (500 volt), Fig. 19c.

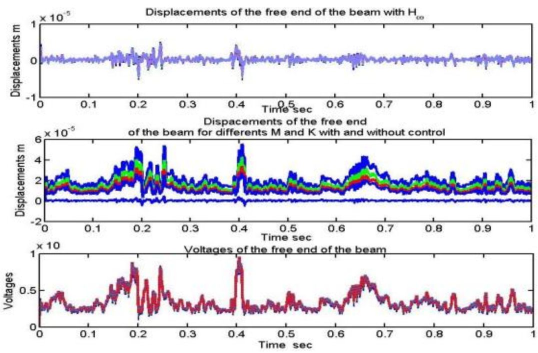

Fig. 18 Variations of nominal mass and stiffness matrices

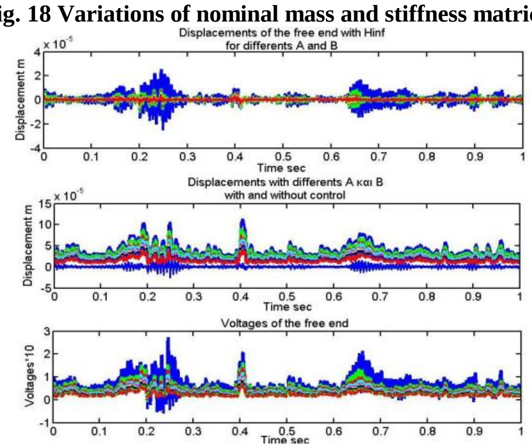

Fig. 19 Variations of nominal matrices A and B.

VII. CONCLUSION

In the present work, the use of active control technology in smart structures has been presented. The goal of control is vibration reduction, while sustaining low steady state error, short recovery time and small maximum uplift; at the same time, control energy must remain within operating limits. The beam that was used was discretized using one-dimensional finite elements with two degrees of freedom per node. Piezoelectric actuators were embedded in it with the objective of reducing vibrations under stochastic loading conditions. We applied more advanced control techniques, such as the H_∞ criterion. The advantage of H_∞ control is the fact that it allows taking into account in the computation the worst case result of disturbances with uncertainty and system noise. Moreover, the H_∞ controller can effectively cope with stronger input, permitting design for a large frequency bandwidth. Results are noteworthy; vibration reduction is observed even for realistic wind loading, with piezoelectric component voltage kept within tolerance. The robust characteristics of the H_∞ controller were then assessed, taking into consideration nonlinearities and system dynamics neglected in modeling, incomplete knowledge of disturbances, environment influence in the form of disturbances, and unreliability of system sensor measurements. Complete vibration reduction was achieved even for variations of beam mass and stiffness up to 50%. H ∞ controller results were very satisfactory and prove that H ∞ control can reduce smart structures vibrations and deal with modeling uncertainty, external disturbances, and noise in measurements.

REFERENCES

[1] B. Bandyopadhyay, T. C. Manjunath, M. Unapathy, "Modeling, Control, and Implementation of Smart Structures," Springer ISBN-10 3-540-48393-4, 2007.

[2] JV. Burke, D. Henron, AS. Kewis, M. L. Overton, "Stabilization via Nonsmooth, Nonconvex Optimization. Automatic Control," IEE. 2006, Vol. 5, Issue 11, pp. 1760–1769, 2006.

[3] S. M. Yang and Y. J. Lee, "Optimization of non collocated sensor, actuator location and feedback gain and control systems. Smart materials and structures," Vol. 8, pp. 96-102, J. 1993.

[4] B. Miara, G. Stavroulakis, V. Valente, "Topics on mathematics for smart systems," Proceedings of the European Conference. Rome, Italy, 26-28 October 2006, World Scientific Publishers, Singapore, International, 2007.

[5] A. Moutsopoulou, A. Pouliezos, G.E. Stavroulakis, "Modeling with Uncertainty and Robust Control of Smart Beams," Paper 35, Proceedings of the Ninth International Conference on Computational Structures Technology. B.H.V. Topping and M. Papadrakakis, (Editors), Civil Comp Press, 2008.

[6] G. E. Stavroulakis, G. Foutsitzi, E. Hadjigeorgiou, D. Marinova, C. C. Baniotopoulos, "Design and robust optimal control of smart beams with application on vibrations

suppression," Advances in Engineering Software, Vol.36, Issues 11-12, pp. 806–813., 2005.

[7] H. F. Tiersten, "Linear Piezoelectric Plate Vibrations," Plenum Press New York, 1969.

[8] N. Zhang and I. Kirpitchenko, "Modeling dynamics of a continuous structure with a piezoelectric sensor/actuator for passive structural control," Journal of Sound and Vibration, Vol. omp Press, Stirlingshire Scotland, Civil Comp Press, Vol. 249, pp. 251–261, 2002.

[9] K. Chandrashekara, S. Varadarajan, "Adaptive shape control of composite beams with piezoelectric actuators," Intelligent Materials Systems and Structures, Vol. 8, pp.112–124, 1997.

[10] Y. H. Lim, V. Senthil Gopinathan, V. Vasundara Varadhan, and K. Vijay Varadan, "Finite element simulation of smart structures using an optimal output feedback controller for vibration and noise control," Int. Journal of Smart Materials and Structures Vol. 8, No. 8, pp.324–337, 1999.

[11] B. Culshaw, "Smart structures : A concept or a reality," Journal of Systems and Control Engg, Vol. 26, No. 206, 1992.

[12] S. Rao, M. Sunar, "Piezoelectricity and its uses in disturbance sensing and control of flexible structures: A survey," Applied mechanics Reu, Vol. 17, No..2, pp. 113-119, 1994.

[13] T. Baily, J. E. Jr. Hubbard, "Distributed piezoelectric polymer active vibration control of a cantilever beam," Journal of Guidance, Dynamics and Control, Vol. 8, No. 5, pp. 605-611, 1985.

[14] S. Hanagud, M. W. Obal, and A. J. Callise, "Optimal vibration control by the use of piezoelectric sensors and actuators," J. Contr. Guidance, Vol. 15, No. 5, pp.1199-1206, . 1992.

[15] Woo Seok Hwang and Hyun Chul Park, "Finite element modeling of piezoelectric sensors and actuators," AIAA journal J, Vol. 31, No. 5, pp. 930-937, 1993.

[16] B. Bona, M. Indri, A. Tornamble, "Flexible piezoelectric structures approximate motion equations and control algorithms," IEEE Auto. Contr., Vol. AC-42, No. 1, pp. 94-101, 1997.

[17] W. Schiehlen, and H. Schonerstedt, "Controller design for the active vibration damping of beam structure," Proc. Smart Mechanical Systems Adaptronics SAE International. USA, pp. 137-146, 1998.

[18] Seung-Bok Choi, Chae-Cheon Cheong, and Chul-Hea Lee, "Position tracking control of a smart flexible structure featuring a piezofilm actuator," Journal of Guidance and Control, Vol. 19, No. 6 , pp. 1364-1369, 1996.

[19] Forouza Pourki, "Distributed controllers for flexible structures using piezoelectric actuators/ sensors," Proc. 32nd IEEE CDC Conf., Texas, USA, pp. 1367-1369, DEC. 1993.

[20] A. Benjeddou, MA. Trindade, R. Ohayon, "New shear actuated smart structure beam finite element," Journal of Guidance, Dynamics and Control, Vol. 37, pp. 378-383, 1999.

[21] X. D. Zhang, C. T. Sun, "Formulation of an adaptive sandwich beam," Smart Materials and Structures Journal, Vol. 5, No. 6, pp. 814-823, 1996.

[22] S. Raja, G. Prathap, P.K. Sinha, "Active vibration control of composite sandwich beams with piezoelectric extension-bending and shear actuators," J. Smart Materials and Structures, Vol. 11, No. 1, pp. 63-71, . 2002.

[23] J. Friedman, K. Kosmatka, "An improved two node Timoshenko beam finite element," J. Computer and Structures, Vol. 47, pp. 473-481, 1993.

[24] X. Zhang, C. Shao, S. Li, D. Xu, "Robust H∞ vibration control for flexible linkage mechanism systems with piezoelectric sensors and actuators," J.l of Sound and Vibration, Vol. 243, No. 1, pp. 145-155, 2001.

[25] A. Packard, J. Doyle, and G. Balas, "Linear, multivariable robust control with a μ perspective," ASME Journal of Dynamic Systems, Measurement and Control, 50th Anniversary Issue, Vol. 115, No. 2b, pp. 310–319, 1993.

[26] B. A. Francis, "A course on H∞ control theory," Springer – Verlag, 1987.

[27] J. C. Doyle, K. Glover, P. Khargoneker, and B. Francis, "State space solutions to standard h2 and h∞ control problems," IEE Trans. Automatic Control 34, pp. 831–847.

[28] H. Kwakernaak, "Robust control and H∞ optimization," Tutorial hper JFAC. Automatic, Vol. 29, No. 2, pp.255-273, 1993.

[29] G. Zames, "Feedback minimax sensitivity and optimal robustness," IEE Trans. Autom. Control, Vol. 28, pp. 585–601, 1983.

[30] H. Kimura, "Robust stability for a class of transfer functions," IEE Transactions on Automatic Control 29, pp. 788–793, 1984.

AUTHOR'S PROFILE

Amalia J. Moutsopoulou was born on the 24th of March 1972 in Athens and she is married with three children. She was graduated Civil Engineer in Democritus University of Thrace. She received her Diploma (M.Sc.) in Construction management and her Doctorate (Ph.D.) in Mechanical and Control engineering, in 1999 and 2009 , respectively, both from the Technical University of Crete in the Department of Production Engineering and Management..

She is associate professor in Technological Educational Institute of Crete, in the department of the Civil Engineering and she teaches Reinforced Concrete Constructions and Building Constructions, from 1997 until today. She has written three books and she has many publications in international journals and conferences, her research interests include mechanical and control engineering. She speaks three languages, French, German and English.

Georgios E. Stavroulakis was born on the 8th of February 1963 in Chania and he is married with three children. He obtained the Civil Engineering Diploma and PhD, both from the Aristotle University of Thessaloniki in 1985 and 1991, respectively, as well as the 'venia legendi' in Mechanics from the Carolo Wilhelmina Technical University of Braunschweig in 2000.

He is currently professor at the Department of Production Engineering and Management at the Technical University of Crete and visiting lecturer (Privatdozent) at the Department of Civil Engineering at the Technical University of Braunschweig. The research work of Dr. Stavroulakis and his co-workers in the areas of computational and contact mechanics, structural optimization and inverse problems and smart

ISSN: 2277-3754
ISO 9001:2008 Certified
International Journal of Engineering and Innovative Technology (IJEIT)
Volume 3, Issue 3, September 2013

structures has been presented in four international monographs and numerous publications. Further details can be found in the Institute's web page www.comeco.tuc.gr .

Anastasios Pouliezos was born in Athens. He received the BSc. Degree in Mathematics and Computing from the Polytechnic of North London in 1975, MSc. in Control Systems from Imperial College, University of London in 1976 and Phd. degree from Brunel University London in 1980.

He is full professor of Control Systems at the Department of Production and Management Engineering of the Technical University of Crete, Greece. Since 1985 a member of the academic staff of the Technical University of Crete. He is the Director of the Industrial Systems Control Laboratory of the Technical University of Crete, which is built around a team of experts and specializes, amongst others, in the areas of automatic control, system fault diagnosis, on-line quality control, on-line health condition monitoring, e-learning, intelligent energy systems, intelligent building systems (BEMS), renewable energy sources, transportation and public utility networks, dynamic optimization algorithms. Dr. Pouliezos published over 100 papers in international journals and conference proceedings in the fields of intelligent control, fuzzy and neural systems for prediction and control, decision support systems, on-line quality control, on-line health condition monitoring, e-learning and intelligent building systems (BEMS)..

.